

The Interplay of Disorder and Thermal Fluctuations in Strongly Coupled Electron-Phonon Systems

Sanjeev Kumar and Pinaki Majumdar
 Harish-Chandra Research Institute,
 Chhatnag Road, Jhusi, Allahabad 211 019, India
 (June 3, 2004)

We solve the disordered Holstein model in three dimension considering the phonon degrees of freedom to be classical. We map out the various phases of the 'clean' strong coupling problem, study the formation and 'melting' of the charge ordered (CO) state with temperature (T) and electron density, and uncover a wide regime of phase separation between the CO state and the Fermi liquid. We then quantify the effect of moderate disorder at strong coupling. In the metallic regime, the interplay of disorder and electron-phonon coupling (i) enormously enhances the resistivity (ρ) at $T = 0$, (ii) suppresses the temperature dependent increase of ρ , and (iii) leads to a regime with $d\rho/dT < 0$. Close to half-filling, the CO phase is rapidly suppressed with increasing disorder. These effects underlie phenomena in materials ranging from the A-15 compounds to transition metal oxides.

The effect of electron-phonon (EP) interactions in weak coupling systems is well understood and can be captured within Boltzmann transport theory [1]. However, there are materials, e.g, the A-15 compounds, where the EP coupling is large and the interplay of disorder and EP interaction leads to several unusual features [2-6] in the resistivity, ρ , including a rapid rise in the residual resistivity at weak disorder, suppression of the temperature (T) dependence of ρ and, sometimes, a regime with $d\rho/dT < 0$. Apart from these anomalies in "metallic" systems, strong EP coupling can lead to polaron formation and charge ordering (CO) instabilities, as seen, for example, in the manganites [7] and the nickelates [8,9]. The first order phase boundary between the strong coupling CO phase and the Fermi liquid can lead to phase separation. Disorder acting in this regime disrupts the CO phase and converts the regime of phase separation to one of cluster coexistence of CO domains [10].

This wide range of effects have a common origin in the interplay of strong EP coupling (and the resulting polaronic tendency), with quenched disorder and thermal fluctuations. However, to capture these effects within a unified framework we need to handle the strong coupling and quenched disorder non perturbatively, retain the spatial correlations in the problem, and access transport properties without making ad hoc approximations. Although the literature on electron-phonon systems is vast, such calculations have not been possible till now.

In this paper we study the Holstein model in three dimension with arbitrary coupling and quenched disorder, through a new real space Monte Carlo (MC) technique [11], explicitly retaining the spatial correlations and localisation effects in the problem. We work with adiabatic phonons, i.e treat the phonons as annealed classical degrees of freedom. Apart from demonstrating a powerful new many body technique, our principal results are (i) the amplification of quenched disorder by strong EP

coupling, and the dramatic increase in residual resistivity with weak disorder, (ii) the rapid suppression of the thermal component of $\rho(T)$ with increasing disorder, and (iii) the emergence of a regime with $d\rho/dT < 0$.

Model: The disordered Holstein (d-H) model with spinless fermions and classical phonons is described by:

$$H = \sum_{ij} t_{ij} c_i^\dagger c_j + \sum_i (\epsilon_i - \epsilon) n_i + \sum_i g_i n_i x_i + H_K \quad (1)$$

The t_{ij} are nearest neighbour hopping on a simple cubic lattice, ϵ_i is the quenched binary disorder, with value $\pm t$, ϵ is the chemical potential, g_i is the EP interaction, coupling electron density n_i to the local distortion x_i , and the 'restoring force' arises from $H_K = \sum_i (K/2) x_i^2$. The parameters in the problem are t , ϵ , ϵ , electron density n , and temperature T . We measure energy, frequency, T , etc, in units of t , and use $K = 1$.

While the strong coupling problem with one electron has been widely studied, we do not know of controlled approximations to handle strong coupling at metallic densities, except within dynamical mean field theory (DMFT). Earlier studies have used DMFT in the adiabatic limit [12] to map out the Fermi liquid and polaronic insulator regime, followed by results on the charge ordered (CO) phase [13,14]. The impact of strong EP coupling on $\rho(T)$ and the effect of weak disorder on such a system has also been explored within DMFT [15].

Our present understanding of strong coupling EP systems owe much to DMFT, but there are serious limitations of this approach, particularly in the presence of disorder, (i) disorder and strong EP interactions reinforce each other, tending to generate a strong local correlation between ϵ_i and x_i , inaccessible in the statistically homogeneous description of DMFT, (ii) in such a system the conductivity can no longer be computed in terms of the single particle self energy, as in DMFT, and vertex corrections leading to localisation are crucial, and (iii) the

phase coexistence window, wide at strong coupling, is converted into a CO cluster phase with short range order. This effect, as also the impact of disorder on the CO phase itself is beyond a single site approximation.

With the possibility of polaron formation, and the need to handle disorder and thermal fluctuations, MC calculation is the only unbiased method for approaching the d-FL problem. However, the cost of annealing the phonon variables, via the standard exact diagonalisation based MC (ED-MC) grows rapidly with system size. For a cube with $N = L^3$, the ED-MC cost grows as N^4 , allowing typically $L = 4$ with current resources. We instead use a "travelling cluster approximation" (TCA) [11] for annealing the phonons. Since TCA avoids iterative diagonalisation of the full Hamiltonian, and estimates the energy cost of MC moves based on a smaller cluster Hamiltonian, we can access sizes up to 12^3 with relative ease. We use a 4^3 cluster for the TCA based updates. Once the phonon variables are equilibrated, we diagonalise the full Hamiltonian in the equilibrium configurations to compute [16] electronic properties. We use $N = 8^3$, checking with 10^3 for size effects. Our resistivity is in units of $\hbar a_0 = (\hbar^2 / e^2)$, where a_0 is the lattice spacing.

Let us start with the phases. In the absence of disorder, the finite T phases can be broadly classified as (i) Fermi liquid (FL) with $d = dT > 0$, (ii) a polaronic liquid (PL), with 'large' lattice distortions, no long range positional order, and $d = dT < 0$, and (iii) the charge ordered insulator (COI) state. Unlike at $T = 0$, [17] all the phases have finite density of states (DOS) at the Fermi level. There is no 'phase boundary' between FL and PL and the distinction is only in terms of transport properties.

For $\lambda < 2.0$, Fig.1.(a), the only feature in the $n - T$

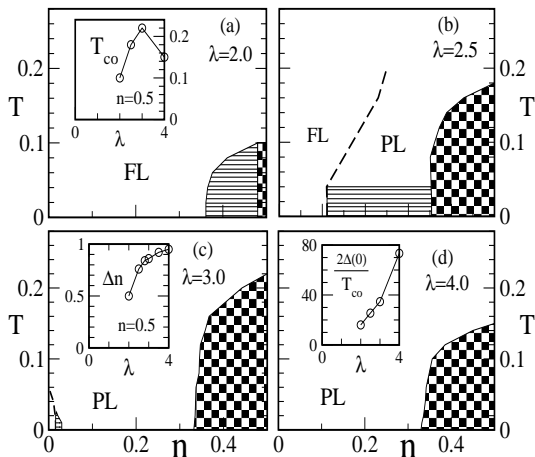


FIG. 1. Phase diagram: clean model. Panels (a) - (d): show the $n - T$ phase diagram with increasing λ . The "chessboard" pattern represents a f ; ; g CO phase, and the hatched regions indicate phase separation. Inset to panel (a): $T_{co}(n)$ at $n = 0.5$, inset to panel (c): charge contrast at $T = 0; n = 0.5$, inset to panel (d): $2 \Delta(n) / T_{co}(n)$ at $n = 0.5$.

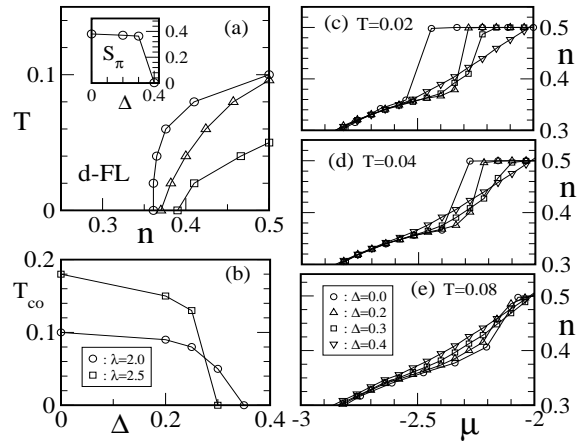


FIG. 2. Phase diagram with disorder. (a): $\lambda = 2.0$, CO at $n = 0.5$ and coexistence region, with increasing disorder: circle = 0, triangle up = 0.2, square = 0.3. Inset CO order parameter at $n = 0.5; T = 0$. (b): $T_{co}(n)$ at $n = 0.5$. (c) - (e): $n(\mu)$ with varying T and Δ , at $\lambda = 2.0$.

phase diagram is the occurrence of CO at $n = 0.5$, and the coexistence region separating the CO phase from the FL. With increasing λ the CO region extends down to $n \approx 0.35$, while T_{co} at $n = 0.5$ grows and then diminishes slowly beyond $\lambda \approx 3.5$. The weak coupling CO instability arises from nesting in the bipartite lattice, with $T_{co} \propto t = E_p$, where $E_p = \sqrt{2(K)}$, while at strong coupling the CO arises from the ordering of 'preformed' polarons, with $T_{co} \propto t = E_p$ [13,14]. The coexistence width at $T = 0$ between the FL and COI increases with increasing λ but the temperature window for coexistence reduces since the finite T strong coupling FL itself has strong density fluctuations. By the time $\lambda = 3.0$ the FL regime has almost vanished, the PL and COI phases dominate the phase diagram, and the system is insulating at all n and T . Our studies will be focused on $\lambda = 2.0$, strong coupling but still metallic, and use $\lambda = 1.0$ as our 'weak coupling' reference. The single polaron threshold is [17] $E_p^c = t = t_c = (2K t) \approx 5.4$, while $\lambda = 2$ leads to $E_p = t = 2$.

The random potential ϵ_i has different effects on the FL and COI phases. For the FL phase it tends to create density inhomogeneities, n_r , which can be strongly amplified depending on λ . This disordered Fermi liquid (d-FL) has unusual transport properties that we discuss later. For the COI phase the disorder couples directly to the order parameter, and acts as a random field. The COI phase has 3d Ising like character and the long range order survives to finite disorder. Fig.2.(a) shows the equivalent of Fig.1.(a), now for $\lambda \leq 0$. Fig.2.(b) shows the dependence $T_{co}(n)$ at $n = 0.5$, and it is seen that the CO phase at $\lambda = 2.5$ disorders at weaker Δ compared to $\lambda = 2.0$. The $n(\mu)$ data in Fig.2.(c) - (e) at $\lambda = 2.0$ shows that the maximum T to which phase coexistence survives is reduced with increasing Δ . This is represented by the bounding curves in Fig.2.(a). At $\Delta = 0.4$ there is no discontinuity in the $n(\mu)$ data at any T , and the f ; ; g

peak in the structure factor also vanishes. As the transport data, Fig.3.(f), and the DOS in Fig.4 indicate, the COI is actually converted into a "metallic" (d-FL) phase by disorder. For $\gamma > 2.5$ disorder converts the COI to a PL [18] without any intervening metallic regime.

The resistivity arises in response to a combination of quenched disorder and lattice distortions. For a phonon configuration \mathbf{x}_i , the potential seen by the electrons is $\phi_i = \phi_i(\mathbf{x}_i)$. Subtracting out the spatial average the fluctuating part is $\phi_i - \bar{\phi} = \phi_i(\mathbf{x}_i - \bar{\mathbf{x}})$. Since the spatially averaged distortion does not depend on configurations, i.e. $\bar{\mathbf{x}} = \bar{\mathbf{x}}$, we can write $\mathbf{x}_i = \bar{\mathbf{x}} + (\mathbf{x}_i - \bar{\mathbf{x}})$, where $\bar{\mathbf{x}}$ is the $T = 0$ distortion at R_i . Defining $\mathbf{x}_i^0 = \bar{\mathbf{x}}$ and $\mathbf{x}_i^1 = \mathbf{x}_i - \bar{\mathbf{x}}$, we obtain $\phi_i = \phi_i(\bar{\mathbf{x}} + \mathbf{x}_i^1)$. Averaging spatially, and over equilibrium configurations, the variance is $\langle \phi_i^2 \rangle = \langle h(\mathbf{x}_i^0)^2 \rangle + 2 \langle h(\mathbf{x}_i^0) \mathbf{x}_i^1 \rangle + \langle h(\mathbf{x}_i^1)^2 \rangle$, say. $\langle \phi_i^2 \rangle_0$ is a measure of disorder at $T = 0$, is a rough measure of "thermal disorder", and $\langle \phi_i^2 \rangle_{\text{corr}}$ locally correlates the thermal fluctuations and $T = 0$ disorder.

In the clean FL $\langle \phi_i^2 \rangle = 2 \langle h(\mathbf{x}_i^0)^2 \rangle$, since $\mathbf{x}_i^0 = 0$. The stiffness to thermal fluctuations of the \mathbf{x}_i , at low T , can be roughly estimated from the energy cost $(K=2)x_i^2 + \frac{1}{2} \langle \phi_i^2 \rangle$, where $\langle \phi_i^2 \rangle$ is the local, zero frequency, density response function of the electron system. The effective stiffness is $K_{\text{eff}} = K + \frac{1}{2} \langle \phi_i^2 \rangle$ leading to $\langle \phi_i^2 \rangle / T = K_{\text{eff}}$. The thermal disorder is $\langle \phi_i^2 \rangle = \frac{1}{2} \langle \phi_i^2 \rangle_0 + \frac{1}{2} \langle \phi_i^2 \rangle_{\text{corr}}$. Electron scattering from these fluctuations would lead to $\rho(T) \propto \frac{1}{T}$, for $T \ll W$ (where $W = 12t$), but as $\frac{1}{T}$ grows the resistivity rises faster than $\frac{1}{T}$, due to localisation corrections, unlike in DMFT [15].

Both the nature of $\langle \phi_i^2 \rangle$ and $\rho(T)$, in the clean metallic case, $n = 0.3$, $\gamma = 1.0$, Fig.3.(a)& (d), and $\gamma = 2.0$, in

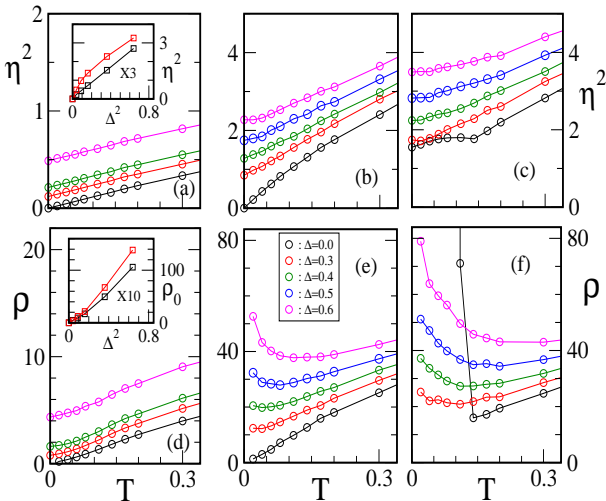


FIG. 3. Effective disorder, $\langle \phi_i^2 \rangle$, and resistivity, $\rho(T)$. (a) (c): shows $\langle \phi_i^2 \rangle$: (a) $\gamma = 1.0; n = 0.3$, (b): $\gamma = 2.0; n = 0.3$, (c): $\gamma = 2.0; n = 0.5$. (d) (f): $\rho(T)$, corresponding to respective panel above. Inset to (a): $\langle \phi_i^2 \rangle$ at $T = 0; n = 0.3$, black $\gamma = 1.0$, red $\gamma = 2.0$, inset to (d): $\rho(0)$ vs ρ_0 at $n = 0.3$, black $\gamma = 1.0$, red $\gamma = 2.0$.

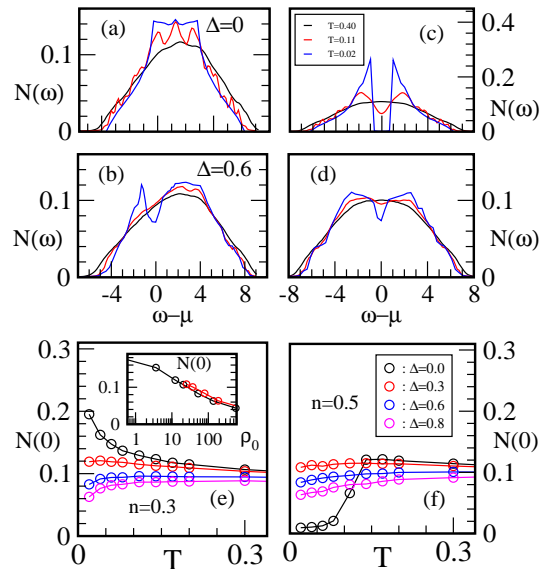


FIG. 4. Density of states, at $\mu = 2.0$. (a) (b): $n = 0.3$, (c) (d): $n = 0.5$. The γ and T are marked on the panels. (e) (f): Variation of $N(0)$, the DOS at E_F , with T : (e): $n = 0.3$, (f): $n = 0.5$. Inset to (e): Correlation, at $T = 0$, $n = 0.3$, between $N(0)$ and ρ_0 , varying γ .

Fig.3.(b)& (e), can be understood within the above scenario. For $n = 0.5$, Fig.3.(c)& (f), which is COI at low T , the resistivity diverges for $T \rightarrow 0$, due to the gap in the DOS, Fig.4.(c). With increasing T , however, $\rho(T)$ displays a minimum after which the resistivity almost follows the $n = 0.3$ result. The naive expectation of activated behaviour $\rho(T) \propto e^{(0)/T}$, where (0) is the $T = 0$ single particle gap, does not bear out since the COI gap itself collapses rapidly with T leaving only a weak pseudogap by the time $T = T_{c0}$. This happens despite the strongly non-mean field ratio $(0)/T_{c0} \approx 16$.

For $\gamma \neq 0$ and $T = 0$, $\langle \phi_i^2 \rangle = \frac{1}{2} \langle h(\mathbf{x}_i^0)^2 \rangle$. If \mathbf{x}_i^0 is small, as one expects at weak disorder and weak coupling, then $\langle \phi_i^2 \rangle \propto \langle \mathbf{x}_i^0 \rangle^2$, leading to $(0) \propto \langle \mathbf{x}_i^0 \rangle^2$. We have checked this explicitly at $\gamma = 1$, i.e. $E_F = t = 0.5$, and $n = 0.3$, Fig.3.(a), and the expected dependence clearly holds. However, when $\gamma = 2$, i.e. $E_F = t = 2$, even weak disorder can create strong density inhomogeneities and induce large quenched distortions [19]. In this regime, $\langle \phi_i^2 \rangle$ is dominated by $\frac{1}{2} \langle h(\mathbf{x}_i^0)^2 \rangle$. Since $\mathbf{x}_i^0 \propto (\gamma K)^{-1} \eta_i^0$, we have $\langle \phi_i^2 \rangle \propto (\gamma K)^{-2} \langle \eta_i^0 \rangle^2$. The density inhomogeneity can be strong, $\langle \eta_i^0 \rangle \propto O(1)$, and the γ^4 factor leads to a huge amplification of the external disorder. The rapid growth in (0) , Fig.3.(d) inset, arises in response to this disorder. When $\gamma = 0.6$, the low temperature DOS at E_F begins to show signs of a weak pseudogap, Fig.4.(b).

While the effect of disorder and thermal fluctuations is additive at weak coupling, $\gamma = 1.0$, Fig.3.(a)& (d), and $\rho(T)$ obeys Mathiessen's rule, the response at $\gamma = 2.0$ is non trivial. The same extrinsic disorder leads to much stronger effective disorder, $\langle \phi_i^2 \rangle(T)$, at $\gamma = 2.0$, compared to $\gamma = 1.0$. In both cases $d^2 = dT > 0$, but the "thermal

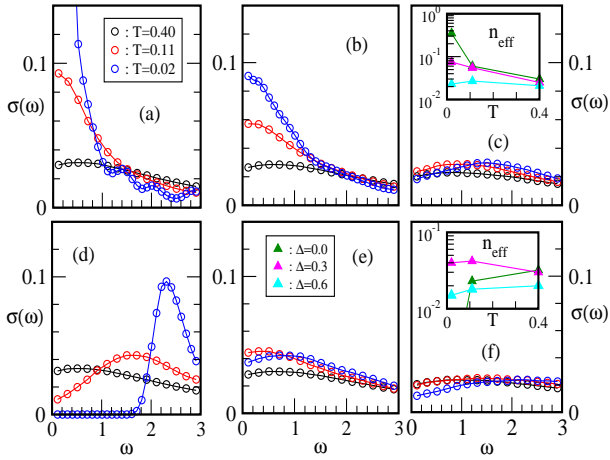


FIG. 5. Optics: $\sigma(\omega)$ at $\omega = 2.0$. (a) (c) are for $n = 0.3$, (d) (f) are for $n = 0.5$. (a) & (d) are for $\Delta = 0$, (b) & (e) $\Delta = 0.3$, (c) & (f) $\Delta = 0.6$. Insets to (c) & (f) show $n_{\text{eff}}(T)$, (c): $n = 0.3$, (f): $n = 0.5$, the legend for insets is in panel (e).

increase" in $\sigma(\omega)$ at $\omega = 2.0$ is actually suppressed with increasing Δ , Fig.3.(d), leading eventually to a regime with $d = dT < 0$, at just $\Delta = 0.6$. These effects arise from the disorder induced polaron formation tendency, at $T = 0$, and its weakening with increasing temperature.

The polaronic localisation effects, (large n_r), which control $\sigma(\omega)$, also lead to a strong suppression in the low frequency optical spectral weight, Fig.5.(c) and inset. The "effective carrier number" $n_{\text{eff}}(\omega; T) = R_0^1(\omega; T)d\omega$, a rough measure of the kinetic energy is reduced by a factor 10 (at $\omega = 1$) as Δ increases from zero to 0.6 at $T = 0$. With increasing T , while n_r^2 increases, the strongly localised particles actually delocalise, as borne out by the increasing DOS at E_F , Fig.4.(b), and $n_{\text{eff}}(T)$, Fig.5.(c): inset. We propose the following approximate "two uid" picture: the electrons in extended states at $T = 0$ contribute to a growing $\sigma(\omega)$, with increasing T , while the localised particles provide a "parallel" conduction channel, with increasing conductivity as T increases. The reduction in $d = dT$ at intermediate Δ comes from these competing tendencies, while for $\Delta > 0.6$ there are few extended states and the delocalising trend dominates. We have explicitly checked the T dependence of n_r , [18], and the density contrast weakens with increasing T . At higher T after the polaronic effects have disappeared $\sigma(\omega)$ again roughly tracks n_r^2 .

There are generic features of real strong coupling EP systems that we can approach based on our simple model. (a): In nominally "clean" $\text{Bi}_{1-x}\text{Ca}_x\text{MnO}_3$, (BCMO), the CO state has been studied via electron diffraction as well as optical reflectivity [20]. The observed T_{CO} is 210-290 K for $x = 0.32 - 0.74$. The large ratio $2 \sigma(0) = T_{CO} / 18 - 24$ suggests strong coupling. The optical gap however does not survive above T_{CO} signifying that the EP coupling, while large, is still below the single polaron threshold. There is also huge transfer of optical spectral weight from high to low frequencies with increas-

ing T , and $n_{\text{eff}}(\omega; T)$ at $\omega = 1$ eV grows rapidly with T (see our Fig.5.(d), and insets). (b): The interplay of disorder and strong EP coupling is best documented in the A-15 compounds [24], where EP coupling is believed to lead to (relatively) high superconducting transition T_{SC} and structural instabilities. The issues of relevance to us are: (i) $\sigma(0)$ increases enormously, in response to disorder (alpha particle damage) [2] compared to similar disorder in a weak coupling material, Nb, say, (ii) as $\sigma(0)$ grows, the thermal increase in $\sigma(\omega)$ is systematically reduced, tending to a limit $d = dT = 0$ at strong disorder [2], (iii) there is a degradation of T_{SC} with increasing $\sigma(0)$, suggesting a possible reduction in the DOS at E_F [3,4]. (iv) Some other systems, e.g. LuRh_4B_4 actually go over to $d = dT < 0$ with increasing $\sigma(0)$ [5,6]. All the features, (i) - (iv) above, find a qualitative explanation in terms of our results. The reduction in DOS inferred from T_{SC} degradation bears a close parallel to our correlation between $N(0)$ and $\sigma(0)$, Fig.4.(e) inset.

Conclusion: We have studied a model involving the interplay of strong EP coupling and disorder using an accurate non perturbative real space method. Our method, and results on transport, spectral features and optics, should be useful in analysing data on materials ranging from the A-15 compounds to transition metal oxides.

We acknowledge use of the Beowulf cluster at H.R.I.

-
- [1] J. M. Ziman, Electrons and Phonons, Oxford University Press, New York (1960).
 - [2] L. R. Testardi et al., Phys. Rev. B 15, 2570 (1977).
 - [3] H. W. Iemann et al., Phys. Rev. B 17, 122 (1978).
 - [4] C. C. Tsuei, Phys. Rev. B 18, 6385 (1978).
 - [5] R. C. Dynes, et al., in Ternary Superconductors, edited by G. K. Shenoy, et al. (North Holland, 1981), pp.169.
 - [6] J. H. Mooji, Phys. Status Solidi, A 17, 521 (1973).
 - [7] Colossal Magnetoresistive Oxides, edited by Y. Tokura, Gordon and Breach, Amsterdam (2000).
 - [8] C. H. Chen, et al., Phys. Rev. Lett. 71, 2461 (1993).
 - [9] J. Zaanen and P. B. Littlewood, Phys. Rev. B 50, 7222 (1994).
 - [10] H. A. Liaga, et al., Phys. Rev. B 68, 104405 (2003).
 - [11] S. Kumar and P. Majumdar, cond-m at 0406082.
 - [12] A. J. Millis, et al., Phys. Rev. B 54, 5389 (1996).
 - [13] S. Ciuchi and F. de Pasquale, Phys. Rev. B 59, 5431 (1999).
 - [14] S. Blawid and A. J. Millis, Phys. Rev. B 62, 2424 (2000).
 - [15] A. J. Millis, et al., Phys. Rev. Lett. 82, 2354 (1999).
 - [16] S. Kumar and P. Majumdar, 0305345.
 - [17] S. Kumar and P. Majumdar, cond-m at 0406083.
 - [18] S. Kumar and P. Majumdar, to be published.
 - [19] D. Emin & M. N. Bussac, Phys. Rev. B 49, 14290 (1994).
 - [20] H. L. Liu, et al., Phys. Rev. Lett. 81, 4684 (1998).